

A Single-Site Platinum CO Oxidation Catalyst in Zeolite KLTL: Microscopic and Spectroscopic Determination of the Locations of the Platinum Atoms**

Joseph D. Kistler, Nutchapon Chotigkrai, Pinghong Xu, Bryan Enderle, Piyasan Praserttham, Cong-Yan Chen, Nigel D. Browning, and Bruce C. Gates*

Abstract: A stable site-isolated mononuclear platinum catalyst with a well-defined structure is presented. Platinum complexes supported in zeolite KLTL were synthesized from $[Pt(NH_3)_4](NO_3)_2$, oxidized at 633 K, and used to catalyze CO oxidation. IR and X-ray absorption spectra and electron micrographs determine the structures and locations of the platinum complexes in the zeolite pores, demonstrate the platinum-support bonding, and show that the platinum remained site isolated after oxidation and catalysis.

Single-site noble metals on metal oxide supports have gained wide attention because of the new opportunities they offer in catalysis.^[1–3] Site-isolated Pt atoms have been observed along with small platinum clusters in catalysts such as those applied in industry at temperatures as high as about 783 K,^[4] and isolated Pt atoms on Al_2O_3 are stable at 533 K.^[5] The metal atoms in some such catalysts have been imaged by aberration-corrected scanning transmission electron microscopy (STEM).^[1–5] Because the support surfaces are nonuniform, the structures of the catalytic species are also nonuniform and challenging to characterize.

In contrast, when the supports are crystalline, they present nearly uniform surface sites for bonding of catalytic species, allowing determination of their locations in the pores, for example, for mononuclear gold in zeolite NaY.^[6] However, this catalyst is unstable at temperatures higher than room temperature, because the gold sinters into clusters.

Now we report a site-isolated noble metal catalyst with a well-defined structure that is stable at high temperatures. The metal is platinum; the support is zeolite LTL. This zeolite was chosen because it is applied industrially as a support for

platinum, present in clusters of only a few atoms each, in catalysts used for alkane dehydrocyclization.^[7] The zeolites in the industrial catalysts are basic, incorporating exchange ions such as K^+ or Ba^{2+} .

Our catalysts were synthesized from zeolite KLTL and aqueous $[Pt(NH_3)_4](NO_3)_2$, resulting in supported $[Pt(NH_3)_4]^{2+}$ complexes,^[8,9] which were oxidized at temperatures as high as 633 K and characterized (by IR, extended X-ray absorption fine structure (EXAFS), and X-ray absorption near-edge structure (XANES) spectroscopies and by STEM) and tested as catalysts for CO oxidation. Experimental details are in Supporting Information. Our goals were to determine the structure and bonding locations of the supported platinum species and to relate catalytic activity to structure.

IR spectra (see the Supporting Information) of the calcined zeolite and the samples made from it indicate that after calcination it contained little water or acidic OH groups, consistent with the initial K/Al atomic ratio of essentially unity, determined by elemental analysis (for details, see the Supporting Information). N–H deformation bands in the IR spectra (1350 and 1390 cm^{-1}) show that $[Pt(NH_3)_4]^{2+}$ complexes were present in the zeolite, as expected.^[10] The bands in the ν_{OH} region representing OH groups in the zeolite framework decreased in intensity upon incorporation and oxidation of the platinum complexes. After oxidation, the band at 3743 cm^{-1} , assigned to zeolite silanol groups,^[11] was the only ν_{OH} band remaining, consistent with the expectation that the platinum complexes had preferentially undergone ion exchange with K^+ ions located near zeolite Al atoms rather than Si atoms.^[12,13]

[*] Dr. J. D. Kistler,^[†] N. Chotigkrai,^[†] P. Xu, Dr. B. Enderle, Prof. Dr. C. Y. Chen, Prof. Dr. B. C. Gates
Department of Chemical Engineering and Materials Science
University of California, Davis
One Shields Avenue, Davis, CA 95616 (USA)
E-mail: bcgates@ucdavis.edu
Prof. Dr. C. Y. Chen
Chevron Energy Technology Company, Richmond, CA 94802 (USA)
Prof. Dr. N. D. Browning
Fundamental and Computational Sciences Division, Pacific Northwest National Laboratory, Richland, WA 99352 (USA)
N. Chotigkrai,^[†] Prof. Dr. P. Praserttham
Center of Excellence on Catalysis and Catalytic Reaction Engineering, Department of Chemical Engineering
Chulalongkorn University (Thailand)

[†] These authors contributed equally to this work.

[**] This work was supported by the Department of Energy (DOE) Basic Energy Science Grants FG02-04ER15513 and DE-SC0005822 and the Royal Golden Jubilee PhD program of the Thailand research fund. We acknowledge beam time and support of beamline 4–1 at the Stanford Synchrotron Radiation Lightsource (SSRL), supported by DOE, Office of Science, Basic Energy Sciences, Contract DE-AC02-76SF00515. We acknowledge support through the Laboratory Directed Research and Development Program Chemical Imaging Initiative at Pacific Northwest National Laboratory (PNNL) and the Environmental Molecular Sciences Laboratory, a national scientific user facility sponsored by DOE's Office of Biological and Environmental Research at PNNL. PNNL is a multiprogram national laboratory operated by Battelle for DOE under Contract DE-AC05-76L01830.


 Supporting information for this article is available on the WWW under <http://dx.doi.org/10.1002/anie.201403353>.

Table 1: EXAFS parameters^[a] characterizing platinum complexes in KLTL zeolite before and after oxidation.^[b]

Sample	Coordination shell	N	R [Å]	$10^3 \times \Delta\sigma^2$ [Å ²]	ΔE_0 [eV]
Pt(NH ₃) ₄ ²⁺ / KLTL zeolite (as- prepared)	Pt–N	4.0	2.00	4.2	-7.3
	Pt–O _{short}	2.0	2.05	2.3	8.0
	Pt–O _{long}	6.0	2.68	7.0	3.7
	Pt–Al	1.0	3.00	6.5	-11.0
PtO _x / KLTL zeolite (oxi- dized)	Pt–N	0.6	2.00	1.2	-1.8
	Pt–O _{short}	2.8	2.01	8.9	-3.8
	Pt–O _{long}	5.9	2.64	10.5	8.0
	Pt–Al	1.1	3.19	2.6	11.3

[a] Sample before oxidation ($\Delta k = 4.0\text{--}10.6 \text{ \AA}^{-1}$, $\Delta R = 0.8\text{--}3.3 \text{ \AA}$). Sample after oxidation ($\Delta k = 4.1\text{--}11.6 \text{ \AA}^{-1}$, $\Delta R = 0.5\text{--}3.0 \text{ \AA}$). [b] Notation: N, coordination number; R, distance between absorber and backscatterer atoms; $\Delta\sigma^2$, disorder term; ΔE_0 , inner potential correction. Estimated error bounds (accuracies): N, $\pm 20\%$; R, $\pm 0.02 \text{ \AA}$; $\Delta\sigma^2$, $\pm 20\%$; ΔE_0 , $\pm 20\%$, but these values do not pertain to the Pt–Al contributions, for which the errors are greater.

Pt L_{III} edge EXAFS spectra of this catalyst (Table 1; for fitting details, see the Supporting Information) are in accord with the IR data, indicating a Pt–N shell with a coordination number of nearly 4. The Pt–O_{support} coordination number of nearly 2 indicates that each Pt atom was bonded, on average, to two zeolite surface oxygen atoms. The absence of a detectable Pt–Pt shell indicates that the platinum species were mononuclear. The Pt–Al coordination number of nearly 1 confirms that the platinum was present in cation-exchange sites.

XANES spectra of the as-prepared sample and that oxidized in 10% O₂ in He at 633 K indicate Pt L_{III} edge energies of 11 567.2 and 11 566.8 eV, respectively. The former value is greater than that characterizing bulk platinum (11 564 eV) and similar to those characterizing Pt^{II} complexes,^[14] including those supported on Al₂O₃.^[15] The white line intensity and XANES features of the as-prepared sample

at approximately 11 580 eV nearly match those of Pt^{II} tetra-amine complexes.^[15] The white line intensity increased during oxidation (Supporting Information, Figure S3), indicating an increase in the number of oxygen donor atoms without a change in the platinum oxidation state,^[16,17] corresponding to the unchanged edge energy^[18] and the increase from 2 to 3 of the Pt–O coordination number representing oxygen atoms bonded to Pt after the oxidation (Table 1).

When the supported [Pt(NH₃)₄]²⁺ complexes were oxidized in flowing 10% O₂ in He as the temperature was ramped from 298 to 633 K at 3 K min⁻¹, most of the NH₃ ligands were oxidized. IR band intensities show that about 15% of these ligands remained unoxidized after 4 h at 633 K (Supporting Information). We stopped short of further oxidation because our goal was to investigate mononuclear platinum species, and reported results^[19] show that the fully deaminated platinum complex in zeolite NaX underwent autoreduction. As the sample was oxidized, mass spectra of the effluent gases showed that water evolution started at about 323 K and N₂ and NO evolution at 466 K, confirming the oxidation of the ligands (Supporting Information).^[19]

EXAFS data characterizing the oxidized sample PtO_x/KLTL zeolite (Table 1) indicate average Pt–N and Pt–O coordination numbers of 0.6 and nearly 3, respectively, and thus a mixture of oxidized and unoxidized platinum complexes, consistent with the remaining NH₃ deformation bands in the IR spectra and the Pt–O_{long} and Pt–Al coordination numbers of approximately 6 and 1 at distances of 2.6 and 3.2 Å, respectively.

A precise determination of the nuclearity of the platinum species is provided by STEM images (Figure 1), which confirm the absence of platinum clusters and show exclusively site-isolated single Pt atom species both before and after oxidation.

In contrast to images of site-isolated Pt atoms reported previously,^[1,3] ours determine the precise locations within the

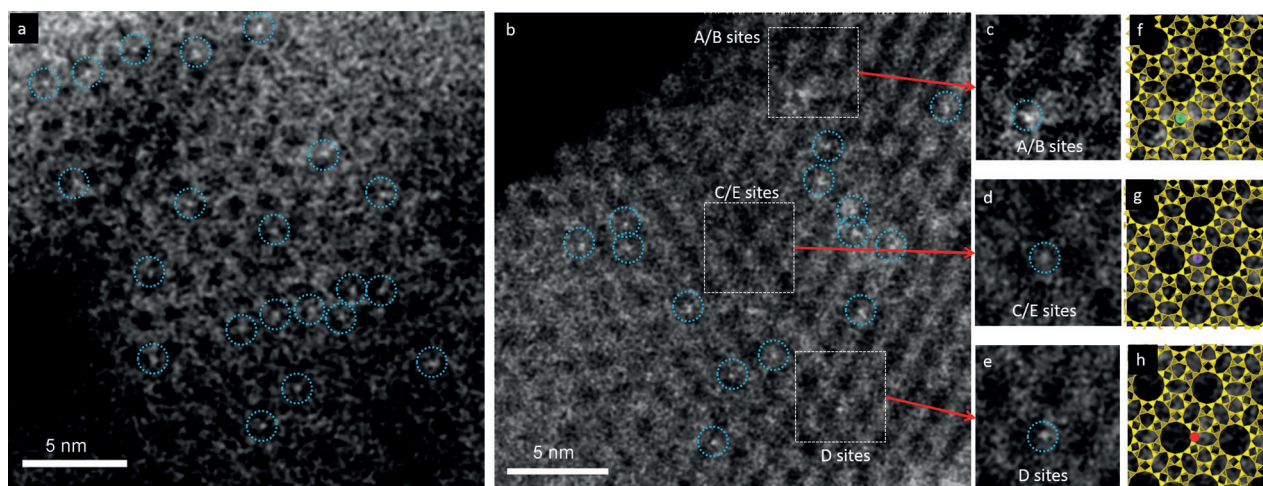


Figure 1. STEM images showing site-isolated Pt atoms in KLTL zeolite in the a) oxidized and b) as-prepared samples. White features in dashed blue circles indicate Pt atoms. Magnified views (c–e) of the highlighted regions in (b), containing one Pt atom each at A/B sites in (c), at C/E sites in (d), and at D sites in (e). Notation is given in the caption of Figure 2. Simulations (f, g) of the LTL zeolite in the [110] direction superimposed on the magnified views in (c–e), showing Pt atoms (green) at A/B sites in (f), at C/E sites in (g) (purple), and at D sites in (h) (red). Pt atoms are located right at the edge of the 12-membered rings of site D; between the two 12-membered rings of sites C/E; and in the center of three 12-membered rings of sites A/B.

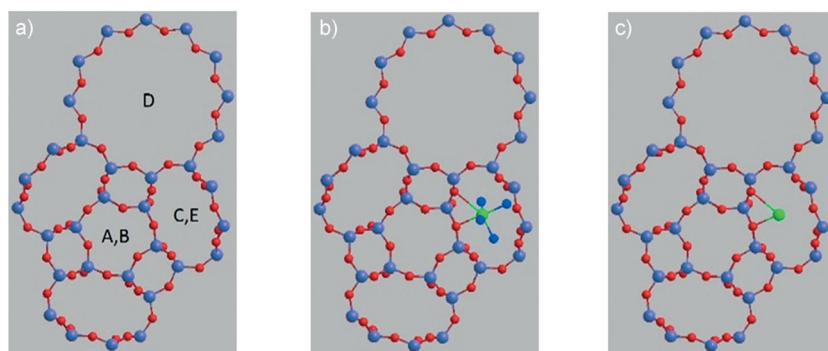


Figure 2. Models of zeolite LTL with a) pore nomenclature as referred to in Figure 1, and b) $[\text{Pt}(\text{NH}_3)_4]^{2+}$ and c) PtO_x located in the 8-membered ring at the C site. The 5 unique bonding locations (A–E) of the Pt atoms are described elsewhere.^[12,13] Pt–O bond distances determined by EXAFS spectroscopy were used with STEM images to determine the Pt atom locations. O red, T-site Si/Al purple, Pt green, N blue; H not shown for clarity. Models depicting the platinum complexes in other pore locations are shown in the Supporting Information.

pore structure of the support. The $[\text{Pt}(\text{NH}_3)_4]^{2+}$ complexes present initially were located primarily in D sites in the largest pores (66%) (Figures 1 and 2). The remainder were in smaller pores, 23% in A/B sites and 11% in C/E sites (notation in caption of Figure 2). Some Pt atoms moved as a result of the oxidation, with the approximate population present in the largest pores decreasing to 56%, that in the medium-sized A/B pores remaining almost unchanged at 24%, and that in the smallest C/E pores increasing to 20%. Details of the STEM calculations are in the Supporting Information. The result confirms previous reports that platinum complexes located in the D sites readily migrate to the E sites upon oxidation.^[12,13]

The EXAFS data show that the surroundings of the Pt atoms, on average, also changed as a result of the oxidation, in agreement with the STEM images. Because the average Pt–O coordination number at the bonding distance of nearly 2.0 Å increased from 2 to nearly 3 (Table 1), we postulate that the oxidation led to the formation of platinum oxo species,^[20] with approximately one oxo O atom per Pt atom, corresponding to the increase in the Pt–O coordination number. These oxo ligands could be stabilized by the lack of significant electron accepting ligands (recall that the zeolite acts as a ligand). Similar results were obtained by EXAFS spectroscopy for a sample made from $[\text{Pt}(\text{NH}_3)_4]^{2+}$ in zeolite NaY oxidized at 633 K.^[8]

The platinum sites in the zeolite were probed with a catalytic test reaction, CO oxidation. The zeolite alone lacked measurable catalytic activity at temperatures up to 423 K, but the platinum-containing zeolite was active both before and after oxidation under conditions described below. The data determine the rate of reaction in each catalyst, measured as turnover frequency (TOF), found by extrapolation of low-conversion data to zero on-stream time. The initial TOF characterizing the as-prepared sample was 0.0038 s^{-1} at 423 K with a feed of 1% CO and 5% O_2 in He; that characterizing the oxidized sample was 0.012 s^{-1} ; our catalysts are among the most active for CO oxidation under our conditions, as shown by the comparison with literature data in the Supporting Information, Table S4. As expected, the

activity of the former catalyst in O_2 increased with time on stream in the flow reactor, as oxo ligands presumably formed and facilitated CO oxidation.^[20]

Furthermore, IR spectra of the catalyst before CO oxidation and recorded after exposure to just CO (see figure in the Supporting Information) gave no evidence of CO adsorption on the coordinatively saturated $[\text{Pt}(\text{NH}_3)_4]^{2+}$ species at 298 K, but the oxidized sample was characterized by a strong, broad CO absorption centered at 2100 cm^{-1} , indicating bonding of CO to the oxidized, catalytically active platinum sites.^[9,20,21]

In summary, the data indicate one of the best-characterized supported platinum catalysts and the first site-isolated platinum catalyst with the locations of the Pt atoms defined. The results demonstrate a strong

advantage of crystalline supports for fundamental understanding of supported catalysts and opportunities for tailoring stable single-site catalysts; they point the way to distinguishing atomically dispersed metal catalysts from metal clusters.

Received: March 14, 2014

Revised: April 30, 2014

Published online: July 1, 2014

Keywords: electron microscopy · EXAFS · platinum · single-site catalysts · zeolites

- [1] M. Flytzani-Stephanopoulos, B. C. Gates, *Annu. Rev. Chem. Biomol. Eng.* **2012**, *3*, 545–574.
- [2] C. Zhang, F. Liu, Y. Zhai, H. Ariga, N. Yi, Y. Liu, K. Asakura, M. Flytzani-Stephanopoulos, H. He, *Angew. Chem. Int. Ed.* **2012**, *51*, 9628–9632; *Angew. Chem.* **2012**, *124*, 9766–9770.
- [3] B. Qiao, A. Wang, X. Yang, L. F. Allard, Z. Jiang, Y. Cui, J. Liu, J. Li, T. Zhang, *Nat. Chem.* **2011**, *3*, 634–641.
- [4] M. M. J. Treacy, *Microporous Mesoporous Mater.* **1999**, *28*, 271–292.
- [5] S. Bradley, W. Sinkler, D. Blom, W. Bigelow, P. M. Voyles, L. F. Allard, *Catal. Lett.* **2012**, *142*, 176–182.
- [6] J. Lu, C. Aydin, N. D. Browning, B. C. Gates, *Angew. Chem. Int. Ed.* **2012**, *51*, 5842–5846; *Angew. Chem.* **2012**, *124*, 5944–5948.
- [7] K. Azzam, G. Jacobs, W. D. Shafer, B. H. Davis, *J. Catal.* **2010**, *270*, 242–248.
- [8] M. S. Tzou, B. K. Teo, W. M. H. Sachtler, *J. Catal.* **1988**, *113*, 220–235.
- [9] Y. Akdogan, C. Vogt, M. Bauer, H. Bertagnolli, L. Giurgiu, E. Roduner, *Phys. Chem. Chem. Phys.* **2008**, *10*, 2952–2963.
- [10] Z. Bastl, M. Beneke, L. Brabec, N. I. Jaeger, P. Hulstede, J. Novakova, G. Schulz-Ekloff, *Phys. Chem. Chem. Phys.* **2000**, *2*, 3099–3104.
- [11] H. Miessner, I. Burkhardt, D. Gutschick, A. Zecchina, C. Morterra, G. Spoto, *J. Chem. Soc. Faraday Trans.* **1989**, *85*, 2113–2126.
- [12] A. Dyer, S. Amini, H. Enamy, H. A. El-Naggar, M. W. Anderson, *Zeolites* **1993**, *13*, 281–290.
- [13] R. Bartolomeu, R. Bertolo, S. Casale, A. Fernandes, C. Henriques, P. da Costa, F. Ribeiro, *Microporous Mesoporous Mater.* **2013**, *169*, 137–147.

- [14] J. T. Miller, M. Schreier, A. J. Kropf, J. R. Regalbuto, *J. Catal.* **2004**, *225*, 203–212.
- [15] A. Munoz-Paez, D. C. Koningsberger, *J. Phys. Chem.* **1995**, *99*, 4193–4204.
- [16] M. D. Hall, H. L. Daly, J. Z. Zhang, M. Zhang, R. A. Alderden, D. Pursche, G. J. Foran, T. W. Hambley, *Metallomics* **2012**, *4*, 568–575.
- [17] S. M. Chen, Y. F. Wu, S. Tao, P. X. Cui, W. S. Chu, X. Chen, Z. Y. Wu, *J. Mol. Struct.* **2013**, *1041*, 39–43.
- [18] K. Takao, S. Takao, A. C. Scheinost, G. Bernhard, C. Hennig, *Inorg. Chim. Acta* **2010**, *363*, 802–806.
- [19] A. C. Camacho Rodrigues, J. L. Fontes Monteiro, *J. Therm. Anal. Calorim.* **2006**, *83*, 451–455.
- [20] I. Efremenko, E. Poverenov, J. M. L. Martin, D. Milstein, *J. Am. Chem. Soc.* **2010**, *132*, 14886–14900.
- [21] K. Chakarova, M. Mihaylov, K. Hadjiivanov, *Microporous Mesoporous Mater.* **2005**, *81*, 305–312.
-